

Complementary metal-oxide-semiconductor compatible athermal silicon nitride/titanium dioxide hybrid micro-ring resonators

Qiu, Feng

Institute for Materials Chemistry and Engineering, Kyushu University

Spring, Andrew M.

Institute for Materials Chemistry and Engineering, Kyushu University

Yu, Feng

Institute for Materials Chemistry and Engineering, Kyushu University

Yokoyama, Shiyoshi

Institute for Materials Chemistry and Engineering, Kyushu University

<https://hdl.handle.net/2324/7238799>

出版情報 : Applied Physics Letters. 102 (5), pp.051106-, 2013-02-06. AIP Publishing

バージョン :

権利関係 : © 2013 American Institute of Physics



RESEARCH ARTICLE | FEBRUARY 06 2013

Complementary metal–oxide–semiconductor compatible athermal silicon nitride/titanium dioxide hybrid micro-ring resonators


Feng Qiu; Andrew M. Spring; Feng Yu; Shiyoshi Yokoyama




Appl. Phys. Lett. 102, 051106 (2013)

<https://doi.org/10.1063/1.4790440>






Lock-in Amplifier



Zurich
Instruments

[Find out more](#)



Boxcar Averager

Boost Your Optics and Photonics Measurements

Complementary metal–oxide–semiconductor compatible athermal silicon nitride/titanium dioxide hybrid micro-ring resonators

Feng Qiu, Andrew M. Spring, Feng Yu, and Shiyoshi Yokoyama^{a)}

*Institute for Materials Chemistry and Engineering, Kyushu University,
6-1 Kasuga-Koen, Kasuga, Fukuoka 816-8580, Japan*

(Received 21 November 2012; accepted 22 January 2013; published online 6 February 2013)

Micro-ring resonators have been widely utilized in silicon photonics. However they often exhibit a high sensitivity to ambient temperature fluctuations. In this letter, we have demonstrated a complementary metal–oxide–semiconductor compatible athermal micro-ring resonator made from titanium dioxide (TiO₂) and silicon nitride (SiN_x). We have exploited the negative thermo-optic coefficient of TiO₂ to counterbalance the positive coefficient of SiN_x. By a precise control over the TiO₂ layer thickness, an athermal condition remarkably consistent with the simulation can be achieved. Therefore, a SiN_x–TiO₂ hybrid micro-ring resonator with a temperature dependent wavelength shift of 0.073 pm/°C has been realized. © 2013 American Institute of Physics. [<http://dx.doi.org/10.1063/1.4790440>]

In recent years, silicon photonics has become the most promising platform within the field of integrated optics. This is due to the materials combination of low fabrication costs, performance enhancements resulting from electronic–photonic integration, and compatibility with the world’s most successful technology for producing electronics, complementary metal–oxide–semiconductor (CMOS).¹ Among many optical waveguide structures in silicon photonics, the micro-ring resonator has the advantages of high device performance, reduced power consumption, and a small device footprint.² A broad range of optical devices, including wavelength filters, wavelength division multiplexers/de-multiplexers, lasers, switches, modulators, and polarization rotators, have been realized by using micro-ring resonators.³

Silicon (Si) and silicon nitride (SiN_x) are two of the fundamental building blocks of current silicon photonics.^{4,5} Due to their high refractive indices, Si and SiN_x micro-ring resonators can have a small radius, a low bending loss, and a high Q-factor. Despite these advantages, Si and SiN_x micro-ring resonators are extremely temperature sensitive because of their narrow resonant spectral width and the thermal-optic effect possessed by the materials. Practically, this means that thermo-electric controllers are required for temperature stabilization, which occupies extra space and consumes more power. There are some methods to realize athermal devices by designing specific waveguide structures without the need for external controllers. Among these methods, the asymmetric Mach–Zehnder interferometer (MZI) waveguide structures and using a polymer cladding layer with compensated thermo-optic (TO) coefficient are the simplest and most easily applicable to devices.^{6,7}

In the first method, a ring resonator is coupled to one arm of a MZI. The guided mode encounters different effective refractive index changes with temperature in the two arms of the MZI, induced by different waveguide widths. By choosing the arm lengths carefully, the temperature sensitivity of one arm

can be set to cancel that of the other, and the temperature dependent wavelength shift (TDWS) can be brought down to zero in theory.^{6,8} This method is CMOS compatible, but the MZI obviously has a larger footprint than that of only a bus-ring resonator. This larger footprint will reduce the degree of integration within silicon photonics. In the second method, a polymer cladding layer is deposited onto a Si or SiN_x core. The polymer has a negative TO coefficient, and the core a positive. Consequently, a temperature independent condition can be achieved when the guided light distributes in the core and the cladding properly.^{2,7} In the case of a Si core, Si has a refractive index of ~ 3.5 and a TO coefficient of $\sim 1.8 \times 10^{-4}/^{\circ}\text{C}$, with the polymer layer usually having a refractive index of ~ 1.45 – 1.6 and a TO of $-(1\text{--}3) \times 10^{-4}/^{\circ}\text{C}$. This requires almost half of the light to be guided in the polymer cladding.⁷ In order to enable more light into the cladding, the dimension of Si core should be highly reduced. This highly reduced dimension usually imposes big challenges for fabrication and results in a large optical loss.⁹ For the SiN_x core case, SiN_x has a refractive index of 1.98 and a TO coefficient of $4 \times 10^{-5}/^{\circ}\text{C}$. As a result, the fabricated waveguide must be precise enough, i.e., within a 10–20 nm tolerance for the SiN_x core dimension as well as the polymer cladding thickness.² This high precision is especially difficult for the polymer cladding layer, which is deposited via spin-coating. For silicon photonics, the most serious problem (for both Si and SiN_x) is that polymers are typically not compatible with CMOS processes due to poor long-term operating stability and temperature issues.⁸

Titanium dioxide (TiO₂) is an excellent candidate as an optical coating material because of numerous desirable properties, such as high transmission in the visible and near infrared regions, strong adhesion, high stability against mechanical abrasion, chemical resistance, and high temperature stability. SiN_x has already been extensively utilized in silicon photonics and has shown an outstanding performance in second harmonic generation and as an optical parametric oscillator in ring resonator structures.^{5,10} Another useful characteristic is its high transparency over a wide range of wavelengths between the visible and near infrared. In this letter, the CMOS-compatible

^{a)} Author to whom correspondence should be addressed. Electronic mail: s_yokoyama@cm.kyushu-u.ac.jp.

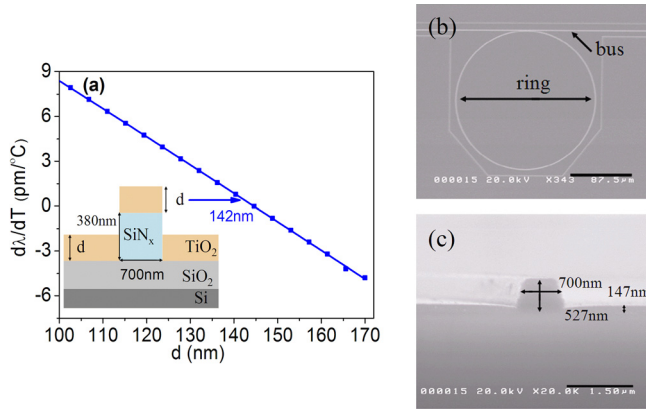


FIG. 1. (a) Calculated TDWS vs TiO_2 layer thickness (inset is the designed waveguide structure). (b) Top view and (c) cross sectional image of the fabricated ring resonator taken by SEM.

and industrial radio frequency (RF) sputtering technique has been applied to deposit a TiO_2 layer onto SiN_x . We have utilized the negative TO coefficient of TiO_2 to counterbalance the positive one of SiN_x to yield CMOS-compatible and small footprint athermal SiN_x - TiO_2 hybrid micro-ring resonators.

The temperature dependence of the resonant wavelength in a ring resonator can be expressed as follows:

$$\frac{d\lambda_m}{dT} = \left(n_{\text{eff}} \cdot a_{\text{sub}} + \frac{dn_{\text{eff}}}{dT} \right) \frac{\lambda_m}{n_g},$$

where λ_m is the resonant wavelength, n_{eff} is the effective refractive index of the waveguide, a_{sub} is the substrate expansion coefficient, and n_g is the group index of the waveguide.^{2,11} An athermal condition is achieved when the $d\lambda_m/dT$ term is zero. To ascertain the optical properties of TiO_2 , we have fabricated and tested TiO_2 ring resonator waveguides. The refractive index of TiO_2 is known to be 2.2 at 1600 nm according to Ref. 12, which was also confirmed by our measurements. The measured TO coefficient of TiO_2 is $-1 \times 10^{-4}/^\circ\text{C}$ from room temperature to 60°C . The choice of the working wavelength is

determined by considering the emission peak of the CMOS-compatible lasers.¹³

Fig. 1(a) shows the calculated TDWS versus the TiO_2 layer thickness d according to the equation and mode calculations using Rsoft.¹⁴ The inset illustrates the designed SiN_x - TiO_2 hybrid waveguide cross-section. From Fig. 1(a), it can be observed that the ring resonator achieves an athermal condition when the TiO_2 thickness d is 142 nm. Our simulations also demonstrate that an error of 10 nm in d can cause a TDWS of $2.0 \text{ pm}/^\circ\text{C}$. A fine control over the TiO_2 thickness is achieved through RF sputtering technique.

The ring resonator was fabricated using electron beam lithography and reactive ion etching on a $\text{SiN}_x/\text{SiO}_2$ ($3 \mu\text{m}$)/Si wafer. The radius of the fabricated ring was measured as $100 \mu\text{m}$ with a bus-ring gap of $0.4 \mu\text{m}$. Subsequently, TiO_2 layers with different thicknesses (from 138 to 153 nm) were deposited onto the etched samples by RF sputtering a TiO_2 target with Ar gas at a speed of 3 nm/min. During the sputtering process, the substrates were maintained at room temperature. Figs. 1(b) and 1(c) show the top view and cross-section of the ring taken by SEM, respectively. The transmission spectra of the resonators were measured using an end-fire coupling system. Light from a tunable laser source (TLS-510, Santec) was coupled into the waveguide in TE mode through a polarization-maintaining lensed fiber and scanned with 20 pm resolution. The sample was placed on a heater in order to manipulate the temperature between 28 and 60°C . Finally the output light from the waveguide was collected using another lensed fiber and detected by a photo-detector to obtain the transmission spectra.

For comparison, we also fabricated a SiN_x ring resonator without a TiO_2 layer (in this case, the bus-ring gap was $0.2 \mu\text{m}$). As shown in Fig. 2(a), the resonance peaks of that ring resonator were measured at 1596.57 nm and 1596.98 nm at 28 and 60°C , respectively. Thus, the TDWS of the SiN_x ring resonator is $12.8 \text{ pm}/^\circ\text{C}$. An optimal athermal condition was achieved in a ring resonator with a 147 nm thick TiO_2

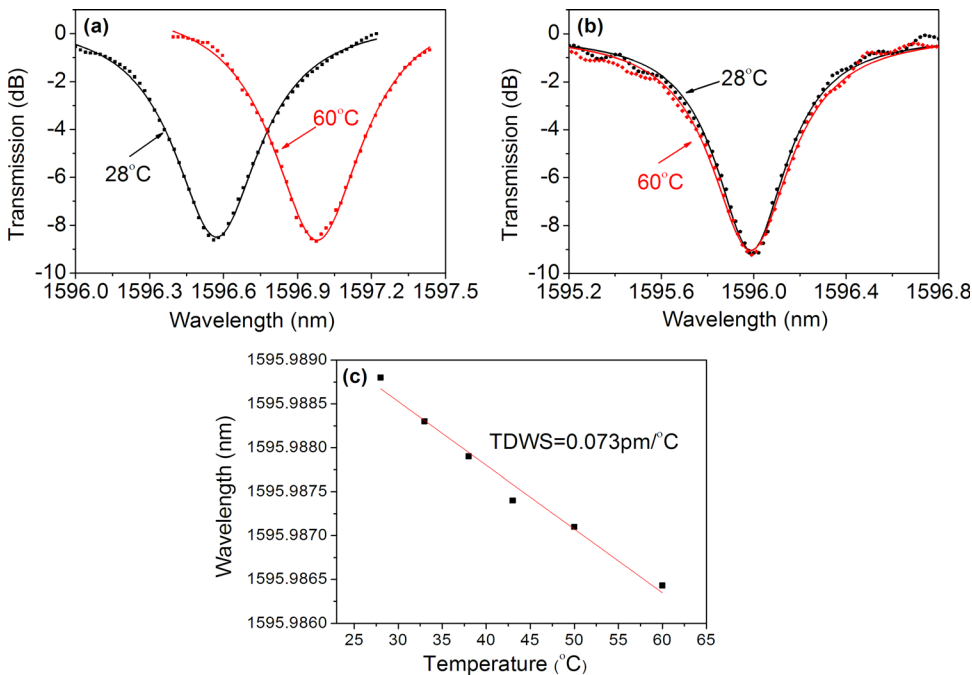


FIG. 2. (a) Transmission spectra of the resonators with $d=0 \text{ nm}$ and (b) with $d=147 \text{ nm}$; (c) the linear fit of TDWS for the ring resonator with $d=147 \text{ nm}$.

layer. Figure 2(b) shows the measured transmission spectra of the SiN_x - TiO_2 hybrid ring resonator at temperatures of 28 and 60 °C. In these spectra, the Lorentz-fitted curves coincide with the measured points. Between these two temperatures, the resonance peak has a 2.4 pm shift and a change of Q value of 350. By the linear fitting of resonance wavelengths at different temperatures in Fig. 2(c), the TDWS of the resonator with $d = 147$ nm is extracted as 0.073 pm/°C. In this study, the values of the TDWSs were obtained from the linear fitting of the data, involving scanning laser resolution, the measured temperature range, and the data points taken into account for linear fitting. These outer factors may have some influence on the value of the TDWS.

For our hybrid resonators, the accuracy of the thickness of the TiO_2 layer can be manipulated to within several nanometers through RF sputtering. This is much more precisely controllable than that achieved by polymer spin-coating and the fabricated dimensions of an asymmetric MZI waveguide.^{6,7} As a result, our demonstrated TDWS of 0.073 pm/°C in this work is enhanced compared to that of the silicon core/polymer cladding ring resonators (0.5 pm/°C and 5 pm/°C),^{7,15} the asymmetric MZI slot SiN_x waveguides (5 pm/°C),¹⁶ and the asymmetric MZI Si waveguides (5 pm/°C).¹⁷ This 0.073 pm/°C TDWS is comparable to our previous work on SiN_x ring resonators with a TDWS of 0.018 pm/°C which was realized by the post-fabrication trimming of the chromophore containing polymer cladding layer.² Additionally, the high chemical and mechanical stability of the TiO_2 layer enables our hybrid resonator to be organic solvent tolerant and high temperature and pressure resistant, compared with much more sensitive polymer claddings. This enables our athermal hybrid resonator to be an excellent candidate for lab-free sensors. The high transparency of TiO_2 and SiN_x over a wide range of wavelengths also makes the resonators very useful in telecommunications technologies, whose window may be extended in future.

In summary, CMOS-compatible hybrid SiN_x - TiO_2 micro-ring resonators have been experimentally demonstrated in this letter. By a fine control over the TiO_2 layer thickness, we have been able to fabricate a hybrid resonator exhibiting a TDWS of 0.073 pm/°C which is almost two orders of magnitude lower than that of the resonator fabricated from only

SiN_x . Furthermore the RF sputtering method used here for TiO_2 deposition may also be applicable to a large range of other commonly used materials, such as silicon, lithium niobate, gallium nitride, and even optical glass. Other temperature sensitive waveguide structures, such as MZI and arrayed waveguide gratings, may be readily fabricated by utilizing this approach.

This work was supported by Nano-Macro Materials, Devices and Systems Research Alliance, Grand-in-Aid for Young Scientists (S), and Global Centers of Excellence Program of the Japanese Ministry of Education, Culture, Sports, Science and Technology. The authors acknowledge the Kitayushu Foundation for the Advancement of Industry.

- ¹G. T. Reed, G. Mashanovich, F. Y. Gardes, and D. J. Thomson, *Nat. Photonics* **4**(8), 518 (2010).
- ²F. Qiu, F. Yu, A. M. Spring, and S. Yokoyama, *Opt. Lett.* **37**(19), 4086 (2012).
- ³A. Chen, H. Sun, A. Pyayt, L. R. Dalton, J. Luo, and A. K. Y. Jen, *IEEE J. Sel. Top. Quantum Electron.* **14**(15), 1281 (2008).
- ⁴B. Jalali and S. Fathpour, *J. Lightwave Technol.* **12**(24), 4600 (2006).
- ⁵J. S. Levy, A. Gondarenko, M. A. Foster, A. C. Turner-Foster, A. L. Gaeta, and M. Lipson, *Nat. Photonics* **4**(1), 37 (2010).
- ⁶B. Guha, B. Kyotoku, and M. Lipson, *Opt. Express* **18**(4), 3487 (2010).
- ⁷J. Teng, P. Dumon, W. Bogaerts, H. Zhang, X. Jian, X. Han, M. Zhao, G. Morthier, and R. Baets, *Opt. Express* **17**(17), 14627 (2009).
- ⁸B. Guha, K. Preston, and M. Lipson, *Opt. Lett.* **37**(12), 2253 (2012).
- ⁹J. M. Lee, D. J. Kim, H. Ahn, S. H. Park, and G. Kim, *J. Lightwave Technol.* **25**(8), 2236 (2007).
- ¹⁰J. S. Levy, M. A. Foster, A. L. Gaeta, and M. Lipson, *Opt. Express* **19**(12), 11415 (2011).
- ¹¹Y. Kokubun, N. Funato, and M. Takizawa, *IEEE Photon. Technol. Lett.* **5**(11), 1297 (1993).
- ¹²M. Furuhashi, M. Fujiwara, T. Ohshiro, M. Tsutsui, K. Matsubara, M. Taniguchi, S. Takeuchi, and T. Kawai, *AIP Adv.* **1**, 032102 (2011).
- ¹³M. J. R. Heck, H.-W. Chen, A. W. Fang, B. R. Koch, D. Liang, H. Park, M. N. Sysak, and J. E. Bowers, *IEEE J. Sel. Top. Quantum Electron.* **17**(2), 333 (2011).
- ¹⁴Rsoft Design Group.
- ¹⁵V. Raghunathan, W. N. Ye, J. Hu, T. Izuhara, J. Michel, and L. C. Kmerling, *Opt. Express* **18**(17), 17631 (2010).
- ¹⁶X. Tu, J. Song, T. Liow, M. K. Park, J. Q. Yiyang, J. S. Kee, M. Yu, and G. Lo, *Opt. Express* **20**(3), 2640 (2012).
- ¹⁷B. Guha, A. Gondarenko, and M. Lipson, *Opt. Express* **18**(3), 1879 (2010).